Express Polymer Letters Vol.17, No.3 (2023) 290–299
Available online at www.expresspolymlett.com
https://doi.org/10.3144/expresspolymlett.2023.21

Research article

Effect of waste zinc oxide particles on properties of natural rubber vulcanizates

Dusadee Tumnantong[1,2], *Pattarapan Prasassarakich*[1,2,3], *Sirilux Poompradub*[1,2,3*]

[1]Department of Chemical Technology, Faculty of Science, Chulalongkorn University, 10330 Bangkok, Thailand
[2]Center of Excellence in Green Materials for Industrial Application, Faculty of Science, Chulalongkorn University, 10330 Bangkok, Thailand
[3]Center of Excellence on Petrochemical and Materials Technology, Chulalongkorn University, 10330 Bangkok, Thailand

Received 21 July 2022; accepted in revised form 30 September 2022

Abstract. Natural rubber (NR) vulcanizates with waste zinc oxide (ZnO) particles were prepared through a sulfur vulcanization process. This research aimed to investigate the effect of different ZnO sources as an activator: commercial ZnO (ZO), waste ZnO obtained from a ceramic industry (WZO), and calcinated WZO (C-WZO) on the properties of NR vulcanizates. The ZnO particles were characterized using X-ray fluorescence spectrometer, X-ray diffractometer, and transmission electron microscopy. It was found that the calcination at 800 °C for 6 h could reduce the sulfur components in WZO; consequently, the particle size and appearance were changed. For rubber vulcanizates, the composition of ZnO in the activator had an effect on the crosslink density of the obtained vulcanizates, resulting in changes to the mechanical tensile, thermal, and dynamic mechanical properties. The crosslink density, tensile strength, and tear strength of the rubber vulcanizate filled with C-WZO (NR/C-WZO (II), 0.18 mmol/cm^3, 21.3 MPa, 68.4 N/mm, respectively) was acceptable for rubber products compared with those of the vulcanizate filled with ZO (NR/ZO, 0.19 mmol/cm^3, 26.4 MPa, 71.6 N/mm, respectively). Accordingly, C-WZO could be used as an effective activator in rubber vulcanization.

Keywords: *rubber, zinc oxide, vulcanization, mechanical properties, thermal properties*

1. Introduction

Natural rubber (NR) is widely used as a polymeric material in various applications such as tires, medical devices, footwear, sports accessories, rubberized coil forms, road rubberization, and so on, because of its unique elasticity and mechanical properties [1, 2]. For practical applications, the raw rubber materials are generally mixed with chemicals and subjected to vulcanization via sulfur or peroxide crosslinking [3]. The long-chain molecules of rubber become chemically joined (cross-linked) to form three-dimensional structures at various points along the chain, which then provide enhanced mechanical properties [4]. In the case of peroxide vulcanization, the mechanical properties of rubber vulcanizates are inferior compared to sulfur vulcanization [5]. The vulcanization of NR with sulfur, originally discovered by Goodyear in 1839, forms sulfur linkages (mono-, di-, and polysulfide bridges) between the polymer chains [6]. Rubber vulcanization in a sulfur system generally uses an accelerator, activator, and co-activator to improve the vulcanization rate and cross-linking efficiency. In the rubber industry, zinc oxide (ZnO) is the most efficient activator for sulfur vulcanization and can reduce the vulcanization time of rubber compounds and enhance the properties of vulcanizates. Therefore, ZnO plays an important role in the transformation of rubber vulcanization [7, 8].

There has not been much research on the effect of ZnO on rubber vulcanization in terms of synthesis,

*Corresponding author, e-mail: sirilux.p@chula.ac.th

properties, and compounding applications. Recently, short prism-like ZnO particles synthesized by a hydrothermal method were compounded with NR latex at different contents to prepare vulcanized NR films that exhibited high mechanical properties [9]. Similarly, the octylamine-capped ZnO nanoparticles with a 5 nm diameter were used in vulcanization to give a high curing efficiency and enhanced mechanical performances of the NR because this structure could improve the ZnO dispersion in the rubber matrix [10]. Active ZnO (3 parts per hundred of rubber [phr]) and nano ZnO (1.5 phr) presented excellent properties for rubber compounds filled with carbon black, which allowed for reduced ZnO usage in forming an elastomeric rubber [11]. For rubber film preparation, ZnO modified with calcium carbonate ($CaCO_3$) at a 9:1 (w/w) ratio effectively activated the NR crosslinking and improved the anti-microbial properties of the rubber products [12]. For styrene-butadiene rubber (SBR) vulcanizates, ZnO nanoparticles (rod-like particles) [13] and rod-like ZnO with different crystal facets [14] were found to give a better vulcanization activity and a good performance with a high crosslink density and a large reduction in the polysulfide crosslinking. In addition, the nanosized ZnO cooperated with ionic liquids [15], while the ZnO nanoparticles prepared by a sol-gel process [16] could reduce the vulcanization time, increase the degree of rubber crosslinking, and improve the tensile properties of the SBR and polyisoprene vulcanizates, respectively. In contrast, ZnO coated on a nano-$CaCO_3$ surface [17], and ZnO dispersed in $CaCO_3$ [18], effectively activated the vulcanization of tire tread compound and ethylene, propylene, and diene monomer elastomer, respectively. For SBR/polybutadiene rubber blends, polyethylene glycol-coated ZnO nanoparticles with a rod-like structure (3 phr) helped to increase the tensile strength of the vulcanizates [19]. These results indicated the importance of investigating the source of ZnO particles in the sulfur vulcanization of rubber.

The ceramic industry has many waste materials during the process [20, 21], so the reuse of ceramic waste has been widely studied in many applications. In ceramic manufacturing, ZnO as glaze coating [22] can ensure crystallization [23], improve the glaze surface properties of floor tiles [24], reduce the coefficient of thermal expansion [25], affect the melting point of the glaze [26], etc. would be one type of ceramic waste. From these mentioned superior properties, the ZnO from ceramic waste is an attractive chemical to substitute for the ZnO as an activator in the vulcanization process. The present work focused on the vulcanization of NR compounds using three different types of ZnO particles as activators, *i.e.*, commercial ZnO (ZO), waste ZnO (WZO) obtained from a ceramic glaze industry, and calcined WZO (C-WZO). To obtain the C-WZO, the WZO was first treated via calcination at 800 °C for 6 h. The physical, thermal, and dynamic mechanical properties of NR vulcanized with the different ZnO types were elucidated.

2. Experimental

2.1. Materials

The NR (STR 5L or Standard Thai Rubber 5L) and curing reagents for rubber compounds: ZO, stearic acid, n-cyclohexyl-2-benzothiazole sulfenamide (CBS), and sulfur, were supplied from the Rubber Research Institute of Thailand. The WZO was obtained from a ceramic glaze industry (Siam Frit Co., Ltd., Samutsakhon, Thailand) and then calcined at 800 °C for 6 h to obtain the C-WZO.

2.2. Preparation of NR vulcanizates

The formulations of the rubber compounds are listed in Table 1. The common rubber compound formula I was filled with 5 phr of ZnO powder and 2.5 phr of sulfur. For the adjusted rubber compound formula II, the actual sulfur content obtained from the ZnO sample and added sulfur was adjusted to be a total of 5 phr. All ingredients were mixed in a two-roll mill at room temperature for 9 min to form NR compounds. Measurement of Mooney viscosity (ML 1+4 at 100 °C) was carried out using Premier™ MV Mooney Viscometer (Alpha Technologies, USA) according to ISO 289-1: 2015. The cure characteristics were determined using a moving die rheometer (MDR, TechPro MD+, USA) at 155 °C following ASTM D5289-19. Optimum cure time (t_{c90}), scorch time (t_{s2}), minimum torque (M_L), maximum torque (M_H) and torque difference ($M_H - M_L$) are presented in Table 1. The sample sheets with dimensions of 150×150×2 mm were prepared at 155 °C and 150 kg/m^2 for 10 min using a compression mold (Scientific LabTech Engineering Co., Ltd., Thailand).

The NR vulcanized samples with ZO, WZO, and C-WZO were denoted as NR/ZO, NR/WZO, and NR/C-WZO, respectively.

Table 1. Formulation of NR compounds in parts per hundred of rubber [phr] and vulcanization parameters.

Sample code	NR/ZO	NR/WZO (I)	NR/WZO (II)	NR/C-WZO (I)	NR/C-WZO (II)
Chemicals					
NR	100.00	100.00	100.00	100.00	100.00
ZO	5.00	0.00	0.00	0.00	0.00
WZO	0.00	5.00	5.58[a]	0.00	0.00
C-WZO	0.00	0.00	0.00	5.00	5.14[a]
Stearic acid	2.00	2.00	2.00	2.00	2.00
CBS	0.60	0.60	0.60	0.60	0.60
Sulfur	2.50	2.50	1.92[b]	2.50	2.36[b]
Cure characteristics					
ML (1+4) at 100 °C	27.0	31.0	30.8	29.5	28.9
t_{c90} [min]	8.72	7.76	7.95	8.53	8.65
t_{s2} [min]	5.34	5.79	5.73	5.67	5.55
M_L [dN·m]	0.43	0.43	0.54	0.43	0.53
M_H [dN·m]	5.62	4.70	4.99	5.12	5.43
$M_H - M_L$ [dN·m]	5.19	4.27	4.45	4.69	4.90

[a]the adjusted WZO or C-WZO and
[b]the adjusted sulfur to make the actual sulfur (2.5 phr)

2.3. Characterization of ZnO

Thermogravimetric analysis (TGA) of the ZO, WZO, and C-WZO was performed using a thermal analysis instrument (Perkin-Elmer Pyris Diamond, USA). The sample (10 mg) was placed on a platinum pan and heated from room temperature to 1000 °C at a constant heating rate of 10 °C/min under nitrogen (N_2) at a flow rate of 50 ml/min. The TGA result was used to find the suitable temperature for WZO calcination.

The X-ray diffraction (XRD) analysis of the different types of ZnO was performed on a Bruker D8 Advance X-ray diffractometer (USA) with CuK_α radiation (λ = 1.54 Å). The X-ray source was operated at 40 kV and 40 mA with a scanning rate of 5–80°, changing at 0.1°/s. The elemental composition was evaluated using wavelength dispersive X-ray fluorescence spectrometry (WDXRF, JEOL Bruker S8 TIGER, USA).

The N_2 adsorption-desorption isotherms of different ZnO samples were measured using a Micromeritics ASAP-2020 surface area and porosity analyzer (USA). The sample (0.15 g) was degassed at 120 °C for 2 h under an N_2 atmosphere to remove the adsorbed moisture. The specific surface area of the samples was evaluated using the Brunauer–Emmett–Teller (BET) method. Theoretical particle size can be determined from the adsorption data and calculated according to Equation (1) [27]:

$$D = \frac{6}{S_{sp} \cdot \rho_a} \quad (1)$$

where D is the theoretical particle diameter [μm], S_{sp} is the specific surface area per unit mass, and ρ_a is the theoretical density of the solid material.

The morphology of ZnO particles was examined using scanning electron microscopy (SEM, JSM-6480LV, Japan) at an acceleration voltage of 15 kV. The samples were first sputter-coated with gold. The morphology of ZnO particles was also obtained using transmission electron microscopy (TEM, JEOL JEM-1400, Japan) operated at an acceleration voltage of 80 kV. A small amount of the sample was dispersed in ethanol solution and the suspension was put on a copper grid.

2.4. Characterization of the NR vulcanizates

The swelling measurement of the NR vulcanizates was determined according to ASTM D471. The sample (10×10×2 mm) was immersed in toluene for 7 d at room temperature. The swelling ratio (Q) of the NR vulcanized samples was then calculated according to Equation (2):

$$Q = \frac{W_2 - W_1}{W_1} \quad (2)$$

where W_1 and W_2 are the weight of the vulcanizates before and after toluene immersion [g], respectively.

The volume fraction (V_r) and crosslink density (η_c) of vulcanizates were determined following Equations (3) and (4), respectively, [28, 29]:

$$V_r = \left[1 + \frac{W_2 - W_1}{W_1} \cdot \frac{\rho_r}{\rho_s}\right]^{-1} \quad (3)$$

$$\eta_c = \frac{-\left[\ln(1 - V_r) + V_r + \chi \cdot V_r^2\right]}{V_s\left[V_r^{1/3} - \frac{V_r}{2}\right]} \quad (4)$$

where ρ_r is the density of the vulcanizates, ρ_s is the density of toluene (0.862 g/cm^3), V_s is the molar volume of toluene (106.4 cm^3/mol), and χ is the NR-toluene interaction parameter (Flory-Huggins value, 0.39) [30].

The mechanical properties of the NR vulcanizates were evaluated using a universal testing machine (Instron 3366, USA) at a 500 mm/min cross-head speed according to ASTM D412. All samples were cut into a dumbbell-type shape. The hardness (Shore A) was measured using the Shore A hardness tester (BAREISS: model Digi test II, USA) according to ASTM D2240. Tear properties and compression set were measured using a universal testing machine (Hounsfield model UTM1T, USA) according to ASTM D624 (die C) and ASTM C165, respectively.

Initial decomposition temperature (T_{id}) and maximum decomposition temperatures (T_{max}) of the NR vulcanizates were measured using thermal analysis (Perkin-Elmer Pyris Diamond, USA). Each sample (10 mg) was placed on a platinum pan and heated from room temperature to 800 °C at a constant heating rate of 10 °C/min under N_2 gas at a flow rate of 50 mL/min.

The glass transition temperature (T_g) of the samples was measured using a dynamic mechanical analyzer (DMA, GABO MODEL: EPLEXOR QC 100, Germany). The temperature was run in the range of –100 to 100 °C at an oscillation frequency of 5 Hz and a heating rate of 2 °C/min. The storage modulus (E') and the loss tangent (tan δ) curves were observed.

3. Results and discussion

3.1. Characterization of ZnO particles

The elemental compositions of ZO, WZO, and C-WZO are presented in Table 2. The commercial ZO had no sulfur components, while the sulfur content in WZO (10.4 wt%) was almost four-fold higher than that in C-WZO (2.7 wt%), indicating that calcining at 800 °C reduced the sulfur components in WZO. Accordingly, the zinc content of the ZnO particles was decreased in the order: ZO (80.3 wt%) > C-WZO (74.9 wt%) > WZO (59.5 wt%). Moreover, these results were supported by the XRD analysis (Figure 1). For the commercial ZO, the characteristic peaks of ZnO were observed without impurity phases. The WZO diffraction peaks consisted of both zinc sulfide (ZnS) and ZnO peaks, according to powder diffraction standards of the Joint Committee on Powder Diffraction Standards (JCPDS) with cards number 36–1450 and 36–1451 [31], respectively. After the calcination of WZO, the XRD patterns presented both ZnS and ZnO peaks, but the intensity of ZnS peaks in C-WZO was lower than that in WZO. The sulfur components (ZnS) of WZO were converted to ZnO during calcination, but the conversion was not complete as it still contained some ZnS.

The TGA thermograms of ZO, WZO, and C-WZO are shown in Figure 2. For the ZO curve, the ZnO weight was 100%, with no significant change. However, the

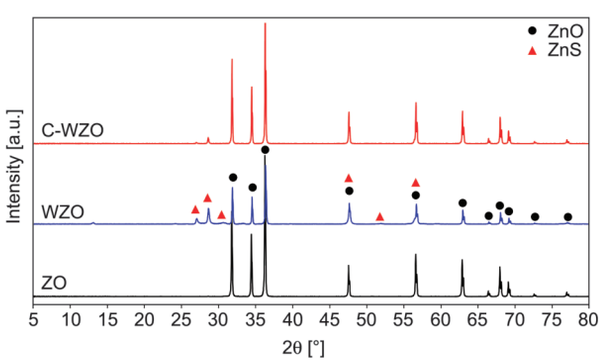

Figure 1. Representative XRD patterns of ZO, WZO, and C-WZO

Table 2. Elemental composition, specific surface area, and particle size of ZO, WZO, and C-WZO.

Sample	Element[a] [wt%]			ZnO[a] [wt%]	Multipoint BET[b] [m^2/g]	Total pore volume[b] [cm^3/g]	Average pore diameter[b] [Å]	Average particle size[b] [nm]
	Zn	S	O					
ZO	80.3	0.0	19.7	100.0	5.33	0.0062	46.6	201
WZO	59.5	10.4	30.0	74.0	3.50	0.0040	45.3	306
C-WZO	74.9	2.7	22.4	93.3	1.93	0.0007	15.0	554

[a]XRF
[b]Surface area and porosity analyzer

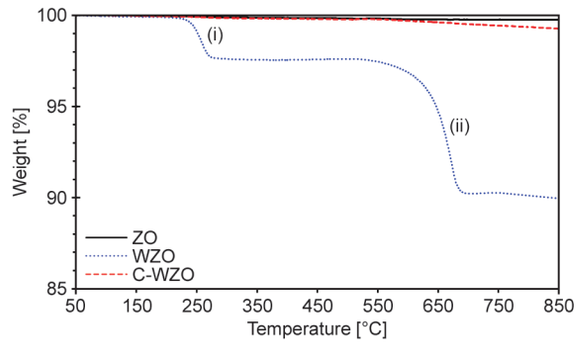

Figure 2. Representative TGA thermograms of ZO, WZO, and C-WZO.

WZO curve presented a two-step degradation with a weight loss of about 2% at 250 °C and a further 7% at 650 °C due to the decomposition of ZnS. It was clearly observed that the C-WZO weight was slightly changed, with a residual weight of 99.5% due to the small loss of light compounds. In accordance with the XRF and XRD analyses, the conversion of ZnS to ZnO proceeded by the oxidation of ZnS to ZnO, and so increasing the ZnO content in C-WZO, as shown in Equations (5) and (6):

$$ZnS\ (s) + 2O_2 \rightarrow ZnO\ (s) + SO_3\ (g) \quad (5)$$

$$2ZnS\ (s) + 3O_2 \rightarrow 2ZnO\ (s) + 2SO_2\ (g) \quad (6)$$

The BET specific surface area and particle size of ZO, WZO, and C-WZO are presented in Table 2. The surface area of WZO (3.50 m^2/g) was less than that of ZO (5.33 m^2/g) because of contamination during the ceramic processing. For C-WZO, the surface area was decreased to 1.93 m^2/g as a result of temperature-induced coalescence during calcination [32]. As mentioned above, the particle size can be calculated from the adsorption data of the surface area and porosity analyzer. The ZO, WZO, and C-WZO had an average particle size of 201, 306, and 554 nm, respectively. These particle size results were in accordance with the SEM and TEM micrographs (Figure 3). The ZO particles (Figure 3a) exhibited a small size with an average size of 200 nm, while the WZO particles (Figure 3b) were slightly larger than the ZO particles. However, C-WZO particles (Figure 3c) were much larger and agglomerated particles compared to the other ZnO samples, which was due to thermal sintering.

3.2. Characterization of NR vulcanizates

The swelling ratio and crosslink density of NR vulcanizates filled with different types of ZnO powder and formula are presented in Table 3. For the formulation of NR compounds, the common rubber compound formula I with WZO or C-WZO and sulfur of 5 and 2.5 phr, respectively, would have the less actual ZnO and higher sulfur than 5 and 2.5 phr, respectively, due to the ZnS amount. For the adjusted rubber compound formula II, the increased WZO or C-WZO (5.58 or 5.14 phr) and decreased sulfur in NR/WZO or NR/C-WZO (1.92 or 2.36 phr) could adjust to the actual sulfur of 2.5 phr in vulcanization system.

The swelling properties related to the crosslink density and the crosslinking of the vulcanized rubber were used to explain the effect of ZnO particles on the vulcanization process. The crosslink density of NR/ZO (0.19 $mmol/cm^3$) was higher than that of NR/C-WZO and NR/WZO due to the high ZnO purity of the ZO sample. Comparing the formula of NR vulcanizates with ZnO powder at 5 phr and sulfur at 2.5 phr, the crosslink density of NR/WZO (I) (0.11 $mmol/cm^3$) was lower than that of NR/C-WZO (I) (0.15 $mmol/cm^3$) due to the lower ZnO content of the NR/WZO sample. WZO and C-WZO had a ZnO content of 74.0 wt% and 93.3%, respectively, corresponding to the crosslink density of their respective vulcanizates. Subsequently, when the actual sulfur content obtained from the WZO or C-WZO and added sulfur was adjusted to be a total of 2.5 phr, the crosslink density of NR/WZO (II) (0.13 $mmol/cm^3$) was also lower than that of NR/C-WZO (II) (0.18 $mmol/cm^3$). These results implied that the sulfur content obtained from the ZnO sample (as ZnS) did not participate in the sulfur vulcanization process. Moreover, the crosslink density of NR/C-WZO (II) and NR/WZO (II) was higher than that of NR/C-WZO (I) and NR/WZO (I), respectively, indicating that the ZnO amount affected the crosslinking of rubber vulcanizates.

The proposed sulfur vulcanization process of the vulcanized rubber filled with different ZnO samples is shown in Figure 4 and is explained as follows. (i) The ZnO component releases zinc ions (Zn^{2+}) that activate sulfur to form the chemical crosslinking of the rubber matrix in the vulcanization process. (ii) Elemental zinc and sulfur in the ZnS were in a non-active structure and did not participate in the rubber sulfur vulcanization. (iii) Sulfur in the S_8 form was suitable to initiate the sulfur crosslinks between rubber chains to create mono-, di- or polysulfide crosslinks. Therefore, the ZnO content of the

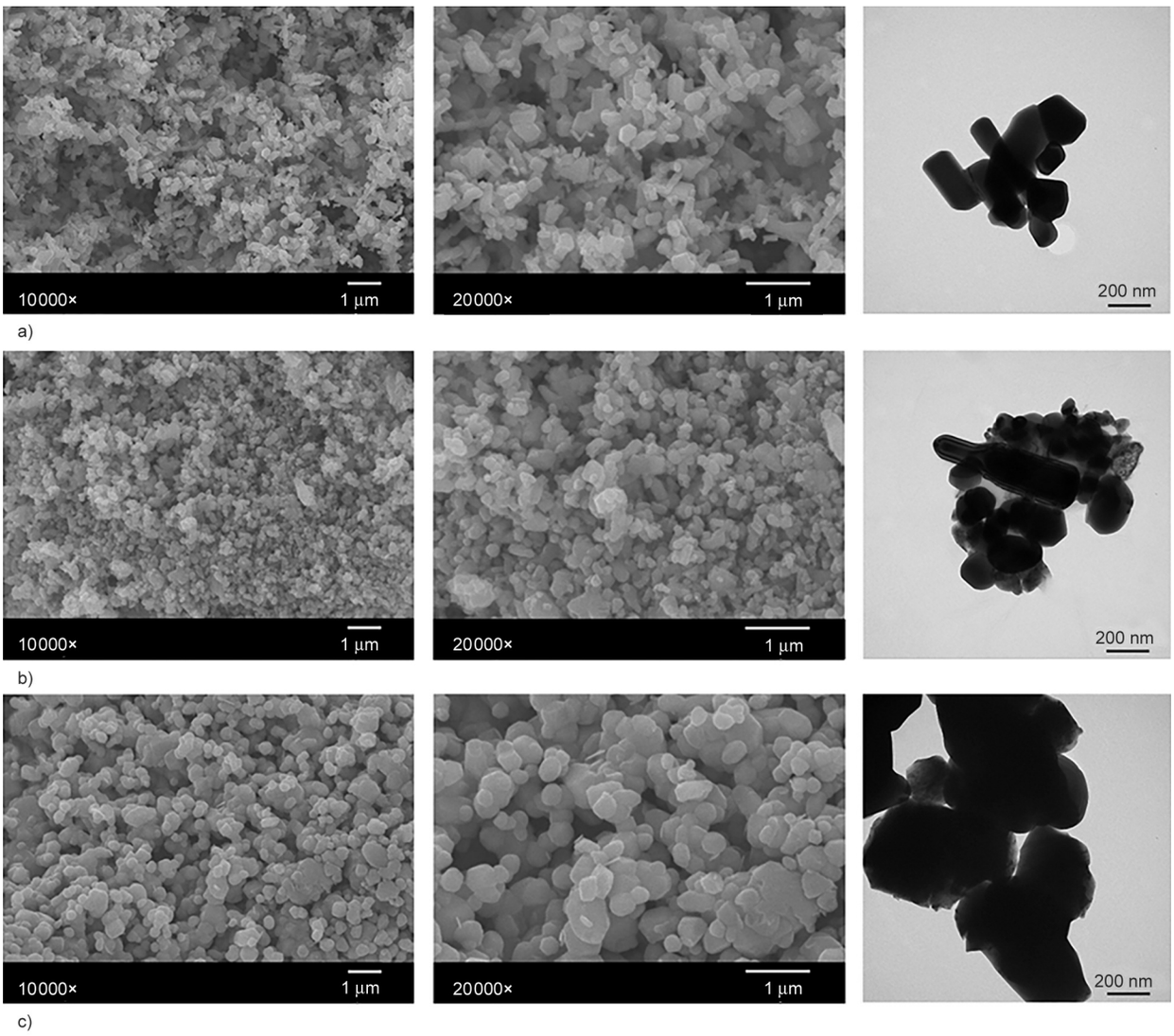

Figure 3. Representative SEM and TEM images of (a) ZO, (b) WZO, and (c) C-WZO.

Table 3. Swelling ratio and crosslink density of NR vulcanizates.

Sample	Swelling ratio [–]	Crosslink density [mmol/cm^3]
NR/ZO	3.31	0.19
NR/WZO (I)	4.52	0.11
NR/WZO (II)	4.05	0.13
NR/C-WZO (I)	3.70	0.15
NR/C-WZO (II)	3.42	0.18

ZO, WZO, and C-WZO particles was a major factor in the NR sulfur vulcanization in this research.

3.3. Physical and thermal properties of the NR vulcanizates

The mechanical properties of the NR vulcanizates are presented in Table 4. The tensile strength of NR/ZO (26.4 MPa) was higher than that of NR/C-WZO and NR/WZO. Comparing the formula of NR

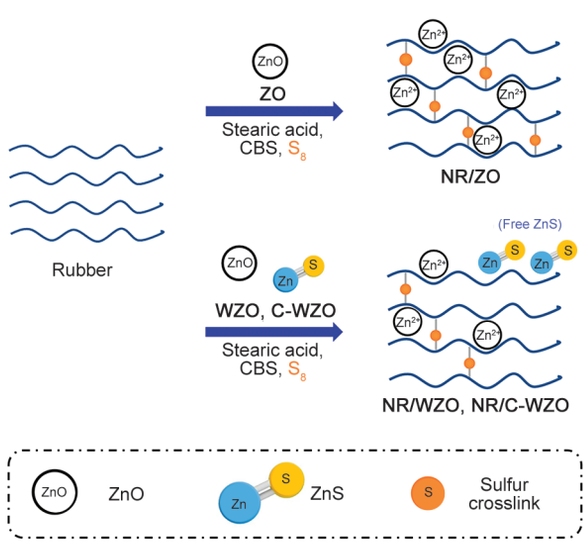

Figure 4. Proposed sulfur vulcanization process of NR vulcanizates.

Table 4. Mechanical properties of NR vulcanizates.

Samples	Tensile strength [MPa]	Elongation at break [%]	100% Modulus [MPa]	300% Modulus [MPa]	Hardness [Shore A]	Tear strength [N/mm]	Compression set [%]
NR/ZO	26.4±1.80	684±16	0.93±0.01	2.49±0.06	40.3±0.3	71.6±3.3	28.1±2.1
NR/WZO (I)	17.1±0.93	693±08	0.76±0.01	1.72±0.03	33.9±0.2	54.2±1.0	25.1±1.0
NR/WZO (II)	16.8±1.18	678±15	0.77±0.02	1.75±0.03	34.8±0.2	63.1±1.5	25.1±1.6
NR/C-WZO (I)	22.0±1.40	677±10	0.89±0.01	2.18±0.06	38.4±0.3	57.1±2.4	24.4±1.2
NR/C-WZO (II)	21.3±2.15	642±20	0.96±0.02	2.45±0.05	39.3±0.2	68.4±1.5	25.1±2.8

Data are shown as the mean±one standard deviation.

vulcanizates with ZnO powder at 5 phr and sulfur at 2.5 phr, the tensile strength of NR/C-WZO (I) (22.0 MPa) was higher than that of NR/WZO (I) (17.1 MPa). When the actual sulfur content obtained from the ZnO sample and added sulfur was adjusted to be a total of 5 phr, the tensile strength of NR/C-WZO (II) (21.3 MPa) was also higher than that of NR/WZO (II) (16.8 MPa). It can be noted that the tensile strength of the NR vulcanizates increased with an increasing crosslink density. In addition, the tensile strength of NR/C-WZO (I) and NR/WZO (I) was about the same (no difference) as those for NR/C-WZO (II) and NR/WZO (II), respectively, while the crosslink density of NR/C-WZO (II) and NR/WZO (II) was higher than that of NR/C-WZO (I) and NR/WZO (I), respectively. This might reflect that some sulfur in the vulcanization system affected the tensile strength of elastomers. Although, the elongation at break of the NR vulcanizates did not show a clear trend, it was quite high in the range of 642–693% due to the elastomeric matrix.

The modulus at 300% strain, hardness, and tear strength of NR/ZO (2.49 MPa, 40.3, 71.6 N/mm) were higher than those of NR/WZO and NR/C-WZO. For the rubber vulcanizates filled with 5 phr ZnO powder and 2.5 phr sulfur, the modulus at 300% strain, hardness, and tear strength of NR/C-WZO (I) (2.18 MPa, 38.4, 57.1 N/mm) were higher than those of NR/WZO (I) (1.72 MPa, 33.9, 54.2 N/mm). For the rubber vulcanizates with an actual sulfur content of 2.5 phr, the modulus at 300% strain, hardness and tear strength of NR/C-WZO (II) (2.45 MPa, 39.3, 68.4 N/mm) were higher than those of NR/WZO (II) (1.75 MPa, 34.8, 63.1 N/mm). In addition, the modulus at 300% strain and hardness of NR/WZO (I) and NR/C-WZO (I) were lower than those of NR/WZO (II) and NR/C-WZO (II), respectively. The modulus at 300% strain and hardness decreased with

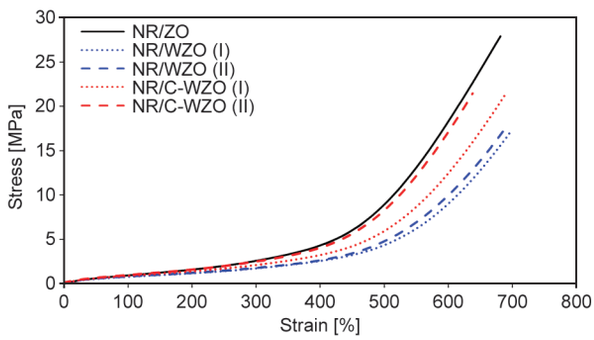

Figure 5. Representative stress–strain curves from the tensile tests of NR vulcanizates.

a decreasing crosslink density due to the restriction on the mobility of rubber chains [33]. Moreover, the compression set of NR/ZO (28.1%) was also higher than that of NR/WZO and NR/C-WZO (24.4–25.1%). Figure 5 shows the stress–strain curves of NR vulcanizates. The rubber vulcanizates had an elastomer behavior with a positive slope and the curve of NR/C-WZO (II) was similar to that of NR/ZO. These results indicated that the C-WZO had a good potential for use as an activator in rubbers with high tensile strength and tear strength (21.3 MPa, 68.4 N/mm) that could be increased by the presence of silica /or carbon black reinforcement in commercial rubber products.

From the thermogravimetric analysis (TGA) and derivative thermogravimetry (DTG) analysis (Figure 6 and Table 5), the NR vulcanizates formed with different types of ZnO all showed a one-step thermal degradation with smooth weight loss. The T_{id} and T_{max} values were in the range of 346.3–348.8 and 375.8–378.4 °C, respectively, corresponding to the decomposition of the NR matrix. Thus, the different types of ZnO (ZO, WZO, and C-WZO) did not influence the thermal stability of the vulcanizates (NR/ZO, NR/C-WZO, and NR/WZO), which retained the same high thermal stability.

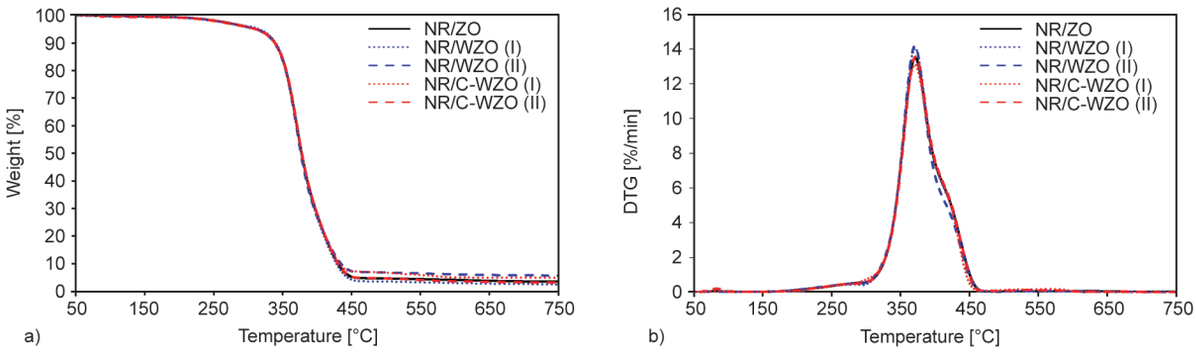

Figure 6. Representative (a) TGA and (b) DTG curves of NR vulcanizates.

Table 5. Thermal and dynamic mechanical properties of NR vulcanizates.

Sample	T_{id} [°C]	T_{max} [°C]	T_g [°C]	E'_{max} [MPa]	$E'_{20\,°C}$ [MPa]	tan δ at the peak [–]
NR/ZO	347.6	377.8	–44.8	2412	1.87	2.41
NR/WZO (I)	348.1	377.7	–45.3	2093	1.67	2.33
NR/WZO (II)	347.5	375.8	–47.4	2295	1.58	2.46
NR/C-WZO (I)	346.3	376.6	–45.0	2417	1.73	2.28
NR/C-WZO (II)	348.8	378.4	–44.4	2409	1.89	2.41

3.4. Dynamic mechanical properties of the NR vulcanizates

The elastic modulus of a polymeric material and its mechanical damping or energy dissipation characteristics as a function of the temperature and frequency can be evaluated by DMA. The storage modulus (E') of the NR vulcanizates is shown in Figure 7 and Table 5. At a low temperature, the E'_{max} value of NR/WZO (2093–2295 MPa) was lower than those of NR/ZO and NR/C-WZO (2409–2417 MPa) due to the presence of ZnS. In addition, the E' values of the vulcanized rubber were decreased around the transition region being a state after the onset of a noticeable reduction in the storage modulus, because the mobility of the polymer chains increased with increasing temperature. Above the glass transition temperature (T_g), the $E'_{20\,°C}$ values of NR/ZO and NR/ C-WZO (1.73–1.89 MPa) were slightly higher than NR/WZO (1.58–1.67 MPa). Therefore, C-WZO could be used as an activator in rubber vulcanization.

The loss tangent (tan δ) of the NR vulcanizates was calculated from the ratio of the dynamic loss modulus (E'') to the storage modulus (E') and is shown in Figure 7 and Table 5. The height of the tan δ curve showed the damping property of the material. The tan δ values of NR vulcanizates were in the range of 2.28–2.46 and were not significantly different. Moreover, the T_g of vulcanized rubber could be determined from the highest value of the tan δ peak. The T_g values of NR/ZO and NR/C-WZO (–44.4 to –45.0 °C) were slightly higher than NR/WZO (–45.3 to –47.4 °C). Thus, the tensile and dynamic mechanical

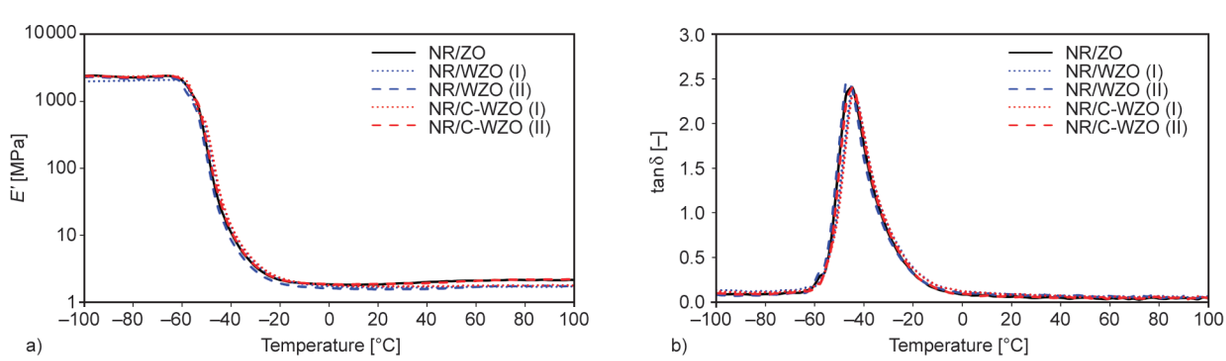

Figure 7. Representative (a) storage modulus (E') and (b) loss tangent (tan δ) of NR vulcanizates.

properties of NR vulcanizates showed the same trend, with C-WZO being an efficient activator in rubber vulcanization.

4. Conclusions

The WZO particles obtained from ceramic processing could be treated via calcination to remove the sulfur components (ZnS). The particle size of WZO and C-WZO was about 1.5 and 2.75-fold larger than the ZO particles, respectively. For NR vulcanizates, the NR/C-WZO had similar physical and dynamic mechanical properties to NR/ZO. As a result of the enhanced crosslink density, the tensile strength, modulus at 300% strain, hardness, tear strength, and storage modulus of NR/C-WZO were superior to NR/WZO. For thermal properties, the rubber vulcanizates with different ZnO particles retained the same high thermal stability. Therefore, C-WZO had the potential to be used as a substance in the sulfur vulcanization process.

Acknowledgements

The authors gratefully acknowledge the support from the Ratchadapisek Somphot Fund for Postdoctoral Fellowship, Chulalongkorn University, and the Center of Excellence in Green Materials for Industrial Application, Chulalongkorn University. The authors also thank Siam Frit Co., Ltd., Samutsakhon, Thailand for raw material support, and Dr. Robert Butcher for editing the article and suggestions.

References

[1] Ikeda Y., Kato A., Kohjiya S., Nakajima Y.: Rubber science. Springer, Singapore (2018).

[2] Thomas S., Chan C. H., Pothen L., Joy J., Maria H.: Natural rubber materials: Volume 2: Composites and nanocomposites. Royal Society of Chemistry, Cambridge (2013). https://doi.org/10.1039/9781849737654

[3] Kruželák J., Sýkora R., Hudec I.: Sulphur and peroxide vulcanisation of rubber compounds – Overview. Chemical Papers, **70**, 1533–1555 (2016). https://doi.org/10.1515/chempap-2016-0093

[4] Schaefer R. J.: Mechanical properties of rubber. in 'Harris' shock and vibration handbook' (eds.: Piersol A., Paez T.) McGraw-Hill, Woodland Hills, 1–18 (2010).

[5] Kruželák J., Hložeková K., Kvasničáková A., Tomanová K., Hudec I.: Application of sulfur and peroxide curing systems for cross-linking of rubber composites filled with calcium lignosulfonate. Polymers, **14**, 1921 (2022). https://doi.org/10.3390/polym14091921

[6] Rodgers B.: Rubber compounding: Chemistry and applications. CRC press, New York (2015).

[7] Maciejewska M., Sowińska A., Kucharska J.: Organic zinc salts as pro-ecological activators for sulfur vulcanization of styrene–butadiene rubber. Polymers, **11**, 1723 (2019). https://doi.org/10.3390/polym11101723

[8] Mostoni S., Milana P., Di Credico B., D'Arienzo M., Scotti R.: Zinc-based curing activators: New trends for reducing zinc content in rubber vulcanization process. Catalysts, **9**, 664 (2019). https://doi.org/10.3390/catal9080664

[9] Junlapong K., Suwanboon S., Khaokong C.: Effects of zinc oxide particle shape on properties of a prevulcanized latex. Iranian Polymer Journal, **28**, 325–335 (2019). https://doi.org/10.1007/s13726-019-00702-w

[10] Qin X., Xu H., Zhang G., Wang J., Wang Z., Zhao Y., Wang Z., Tan T., Bockstaller M. R., Zhang L., Matyjaszewski K.: Enhancing the performance of rubber with nano ZnO as activators. ACS Applied Materials and Interfaces, **12**, 48007–48015 (2020). https://doi.org/10.1021/acsami.0c15114

[11] Sreethu T. K., Naskar K.: Zinc oxide with various surface characteristics and its role on mechanical properties, cure-characteristics, and morphological analysis of natural rubber/carbon black composites. Journal of Polymer Research, **28**, 183 (2021). https://doi.org/10.1007/s10965-021-02536-8

[12] Krainoi A., Poomputsa K., Kalkornsurapranee E., Johns J., Songtipya L., Nip R., Nakaramontri Y.: Disinfectant natural rubber films filled with modified zinc oxide nanoparticles: Synergetic effect of mechanical and antibacterial properties. Express Polymer Letters, **15**, 1081–1100 (2021). https://doi.org/10.3144/expresspolymlett.2021.87

[13] Bieliński D. M., Klajn K., Gozdek T., Kruszyński R., Świątkowski M.: Influence of n-ZnO morphology on sulfur crosslinking and properties of styrene-butadiene rubber vulcanizates. Polymers, **13**, 1040 (2021). https://doi.org/10.3390/polym13071040

[14] Cui J., Zhang L., Wu W., Cheng Z., Sun Y., Jiang H., Li C.: Zinc oxide with dominant (1 0 0) facets boosts vulcanization activity. European Polymer Journal, **113**, 148–154 (2019). https://doi.org/10.1016/j.eurpolymj.2019.01.032

[15] Maciejewska M., Zaborski M.: Thermal analysis and mechanical methods applied to studying properties of SBR compounds containing ionic liquids. Polymer Testing, **61**, 349–363 (2017). https://doi.org/10.1016/j.polymertesting.2017.05.041

[16] Abd-Ali N. K.: The effect of cure activator zinc oxide nanoparticles on the mechanical behavior of polyisoprene rubber. Journal of Engineering Science and Technology, **15**, 2051–2061 (2020).

[17] Thaptong P., Boonbumrung A., Jittham P., Sae-oui P.: Potential use of a novel composite zinc oxide as eco-friendly activator in tire tread compound. Journal of Polymer Research, **26**, 226 (2019). https://doi.org/10.1007/s10965-019-1895-1

[18] Gujel A. A., Bandeira M., Menti C., Perondi D., Guégan R., Roesch-Ely M., Giovanela M., Crespo J. S.: Evaluation of vulcanization nanoactivators with low zinc content: Characterization of zinc oxides, cure, physico-mechanical properties, Zn^{2+} release in water and cytotoxic effect of EPDM compositions. Polymer Engineering and Science, **58**, 1800–1809 (2018). https://doi.org/10.1002/pen.24781

[19] Maiti M., Basak G. C., Srivastava V. K., Jasra R. V.: Influence of synthesized nano-ZnO on cure and physico-mechanical properties of SBR/BR blends. International Journal of Industrial Chemistry, **8**, 273–283 (2017). https://doi.org/10.1007/s40090-016-0107-7

[20] Samadi M., Huseien G. F., Mohammadhosseini H., Lee H. S., Lim N. H. A. S., Tahir M. M., Alyousef R.: Waste ceramic as low cost and eco-friendly materials in the production of sustainable mortars. Journal of Cleaner Production, **266**, 121825 (2020). https://doi.org/10.1016/j.jclepro.2020.121825

[21] Skorulska A., Piszko P., Rybak Z., Szymonowicz M., Dobrzyński M.: Review on polymer, ceramic and composite materials for CAD/CAM indirect restorations in dentistry – Application, mechanical characteristics and comparison. Materials, **14**, 1592 (2021). https://doi.org/10.3390/ma14071592

[22] Burleson M.: The ceramic glaze handbook: Materials, techniques, formulas. Lark Books, New York (2003).

[23] Rudkovskaya N. V., Mikhailenko N. Y.: Decorative zinc-containing crystalline glazes for ornamental ceramics (A review). Glass and Ceramics, **58**, 387–390 (2001). https://doi.org/10.1023/A:1014958309094

[24] Yekta B. E., Alizadeh P., Rezazadeh L.: Floor tile glass-ceramic glaze for improvement of glaze surface properties. Journal of the European Ceramic Society, **26**, 3809–3812 (2006). https://doi.org/10.1016/j.jeurceramsoc.2005.12.016

[25] Da Silva R. C., Pianaro S. A., Tebcherani S. M.: Preparation and characterization of glazes from combinations of different industrial wastes. Ceramics International, **38**, 2725–2731 (2012). https://doi.org/10.1016/j.ceramint.2011.11.041

[26] Moezzi A., McDonagh A. M., Cortie M. B.: Zinc oxide particles: Synthesis, properties and applications. Chemical Engineering Journal, **185–186**, 1–22 (2012). https://doi.org/10.1016/j.cej.2012.01.076

[27] Doostmohammadi A., Monshi A., Salehi R., Fathi M. H., Karbasi S., Pieles U., Daniels A. U.: Preparation, chemistry and physical properties of bone-derived hydroxyapatite particles having a negative zeta potential. Materials Chemistry and Physics, **132**, 446–452 (2012). https://doi.org/10.1016/j.matchemphys.2011.11.051

[28] Chongcharoenchaikul T., Miyaji K., Junkong P., Poompradub S., Ikeda Y.: Synergistic effect of cuttlebone particles and non-rubber components on reinforcing ability of natural rubber and synthetic isoprene rubber composites. Journal of Applied Polymer Science, **139**, 52375 (2022). https://doi.org/10.1002/app.52375

[29] Chongcharoenchaikul T., Miyaji K., Junkong P., Poompradub S., Ikeda Y.: Effects of organic components in cuttlebone on the morphological and mechanical properties of peroxide cross-linked cuttlebone/natural rubber composites. RSC Advances, **12**, 13557–13565 (2022). https://doi.org/10.1039/D2RA01885C

[30] Ikeda Y., Higashitani N., Hijikata K., Kokubo Y., Morita Y., Shibayama M., Osaka N., Suzuki T., Endo H., Kohjiya S.: Vulcanization: New focus on a traditional technology by small-angle neutron scattering. Macromolecules, **42**, 2741–2748 (2009). https://doi.org/10.1021/ma802730z

[31] Li H., Zhao K., Tian S., Zeng D., Pang A., Wang X., Xie C.: Origin of the efficient catalytic thermal decomposition of ammonium perchlorate over (2–1–10) facets of ZnO nanosheets: Surface lattice oxygen. RSC Advances, **7**, 40262–40269 (2017). https://doi.org/10.1039/C7RA07906K

[32] Dengo N., De Fazio A. F., Weiss M., Marschall R., Dolcet P., Fanetti M., Gross S.: Thermal evolution of ZnS nanostructures: Effect of oxidation phenomena on structural features and photocatalytical performances. Inorganic Chemistry, **57**, 13104–13114 (2018). https://doi.org/10.1021/acs.inorgchem.8b01101

[33] Zhao F., Bi W., Zhao S.: Influence of crosslink density on mechanical properties of natural rubber vulcanizates. Journal of Macromolecular Science Part B, **50**, 1460–1469 (2011). https://doi.org/10.1080/00222348.2010.507453